Jørgensen, B.B., D'Hondt, S.L., and Miller, D.J. (Eds.)
Proceedings of the Ocean Drilling Program, Scientific Results Volume 201

5. Impact of Long-Term Diagenesis on $\delta^{15}N$ of Organic Matter in Marine Sediments: Sites 1227 and 1230[1]

Maria G. Prokopenko,[2,3] Douglas E. Hammond,[2] Arthur Spivack,[4] and Lowell Stott[2]

ABSTRACT

This study addresses the problem of diagenetic fractionation of $\delta^{15}N$ in sedimentary organic matter by constructing isotopic mass balances for the sedimentary nitrogen and pore water ammonium at two Ocean Drilling Program (ODP) sites, 1227 and 1230. At Site 1230, ammonium production flux integrated through the sedimentary column indicates that >60% of organic matter is lost to decomposition. The $\delta^{15}N$ of pore water ammonium is <0.7‰ different from that of the sedimentary organic matter, which implies that very little isotopic fractionation is associated with degradation of organic matter at this site. The constant $\delta^{15}N$ of the solid-phase sedimentary nitrogen through the whole profile supports this conclusion. Atomic C/N ratios (9–12) indicate that organic matter at this site is primarily of marine origin. At Site 1227, the sedimentary organic matter appears to be a mixture of terrestrial and marine components. Ammonium is ~4‰ heavier than the organic matter. The observed isotopic enrichment of pore water ammonium relative to the sedimentary nitrogen might indicate either the preferential decomposition of isotopically heavier marine fraction of the organic matter, or possibly, a nonsteady-state condition of the ammonium concentration and $\delta^{15}N$ profiles. Interpretation of the results at Site 1227 is further complicated by the contribution of ammonium with $\delta^{15}N$ of ~4‰ that is diffusing upward from Miocene brines.

[1] Prokopenko, M.G., Hammond, D.E., Spivack, A., and Stott, L., 2006. Impact of long-term diagenesis on $\delta^{15}N$ of organic matter in marine sediments: Sites 1227 and 1230. *In* Jørgensen, B.B., D'Hondt, S.L., and Miller, D.J. (Eds.), *Proc. ODP, Sci. Results*, 201, 1–30 [Online]. Available from World Wide Web: <http://www-odp.tamu.edu/publications/201_SR/VOLUME/CHAPTERS/117.PDF>. [Cited YYYY-MM-DD]
[2] Department of Earth Sciences, University of Southern California, 3651 University Avenue, Los Angeles CA 90089-0740, USA.
[3] Present address: Department of Geosciences, Princeton University, Guyot Hall, Washington Road, Princeton NJ 08544, USA. **mprokope@princeton.edu**
[4] Graduate School of Oceanography, University of Rhode Island, Bay Campus, South Ferry Road, Narragansett RI 02882, USA.

Initial receipt: 30 August 2004
Acceptance: 24 July 2006
Web publication: 1 September 2006
Ms 201SR-117

INTRODUCTION

Nitrogen is one of the important limiting nutrients in the ocean (Gruber, 2004; Redfield et al., 1963; Tyrell, 1999). The global carbon cycle, and, consequently, atmospheric CO_2 might be tightly coupled to the nitrogen cycle (Berger and Keir, 1984; Broecker, 1982), and therefore changes in the magnitude of the sinks and sources of fixed nitrogen in the oceans can significantly influence the global climate (Falkowski, 1997; Ganeshram et al., 1995; Sigman et al., 1999; Sigman and Boyle, 2000).

Biological nitrogen fixation, denitrification, and consumption of nitrate by phytoplankton, the major biological processes of the global nitrogen cycle, can each imprint a distinct isotopic signature ($\delta^{15}N$) on oceanic nitrate and on the phytoplankton that assimilate this nitrate as a nitrogen source (Altabet and Francois, 1994; Haug et al., 1998). Changes in ocean circulation and nutrient supply, which occur in response to changes in environmental conditions, affect the relative importance and spatial extent of the major pathways of the nitrogen cycle; these variations may be recorded in the isotopic ratio of marine phytoplankton, making $\delta^{15}N$ of organic matter buried in marine sediments a sensitive paleoceanographic proxy (Altabet et al., 1991; Altabet and McCarthy, 1985; Francois et al., 1992).

A critical question is whether diagenetic processes fractionate nitrogen isotopes in the buried organic matter, and, if they do, what is the sign and magnitude of this fractionation. A detailed review of previous work addressing this question is given in Prokopenko (2004). A brief summary is provided below. A few laboratory studies have directly addressed the effects of degradation on the isotopic composition of organic matter. The principal reaction in protein degradation involves peptide bond rupture by hydrolysis, which is the principal reaction in protein degradation. Silfer et al. (1992) experimentally demonstrated kinetic fractionation of nitrogen isotopes during abiotic peptide bond hydrolysis, leading to a 2‰–4‰ enrichment of ^{15}N in the residual substrate. Macko and Estep (1984) and Macko et al. (1993, 1983, 1986) showed that both peptide bond hydrolysis and deamination result in the enrichment of ^{15}N in the residual material with the fractionation factor of ~4‰. In a series of incubation experiments, Lehmann et al. (2002) showed that degradation of organic matter under aerobic conditions leaves the residual biomass enriched in ^{15}N isotopes, whereas anoxic decomposition of organic matter results in depletion of ^{15}N. He interpreted the latter case as evidence for bacterial growth, accompanied by the assimilation of ammonium into newly formed bacterial biomass because bacteria grown on ammonium as the sole nitrogen source produce biomass significantly depleted in ^{15}N compared to the original substrate (Hoch et al., 1992).

These experimental findings were supported by field observations made a few years later. Sigman et al. (1999), working with the sediments from the Southern Ocean, and Sachs and Repeta (1999), examining the sapropels from the Mediterranean Sea, found evidence of diagenetic alteration of $\delta^{15}N$ in bulk sediment: a 2‰–5‰ positive shift relative to unaltered organic matter. On the other hand, based on their work in coastal sediments, Altabet et al. (1999) and Pride et al. (1999) argued that in the rapidly accumulating organic-rich sediments of the eastern tropical North Pacific, early diagenesis does not affect isotopic

composition of sedimentary organic matter, if a significant fraction of original sedimentary organic matter is preserved.

To summarize, previous research has shown that under some geochemical conditions, bacterial degradation may lead to changes in nitrogen isotopic ratios of preserved organic matter. However, the degree and direction of isotopic fractionation in marine sediments, as well as the factors controlling them, remain poorly understood.

In this study, we address the problem of diagenetic fractionation of nitrogen isotopes by constructing isotopic mass balances for the sedimentary organic nitrogen and pore water ammonium, which is a major metabolic product of organic matter decomposition. If ammonium is not involved in other diagenetic reactions, its isotopic composition should reflect the isotopic composition of organic nitrogen plus fractionation associated with diagenesis. Cores retrieved during Ocean Drilling Program (ODP) expeditions provide a unique opportunity to evaluate the effect of diagenetic processes on the nitrogen isotopic composition of sedimentary organic matter on a time scale of hundreds of thousand years to million years. Here we present the results from two ODP Leg 201 sites, 1230 and 1227, which represent two geochemically distinct environments.

METHODS

Ammonium concentrations and $\delta^{15}N$, as well as the $\delta^{15}N$ of solid phases were determined through the sediment columns recovered from Sites 1227 and 1230. Bulk sediment samples used for isotopic analyses of solids were "squeeze cakes," kept frozen between the time of collection and analyses. Samples were oven-dried at 60°C for 24 hr and then finely ground. Total nitrogen (TN) and total carbon (TC) were measured on a Carlo Erba CHN-2500 elemental analyzer. Total organic carbon (TOC) was estimated from $\delta^{13}C$ of TC by assuming the $\delta^{13}C$ of carbonate is 0‰ and the $\delta^{13}C$ of organic matter is –21‰. TOC content obtained using this approach is in relatively good agreement with the values measured during Leg 112 (**Meister et al.,** this volume).

Pore water was extracted by squeezing (D'Hondt, Jørgensen, Miller, et al., 2003). Pore water samples collected for isotopic analyses were acidified (to pH ~ 4 for Site 1227 samples and pH ~ 1 for Site 1230 samples) and immediately frozen on board the *JOIDES Resolution*. While acidifying vials for samples from Site 1227, the effect of alkalinity was not taken into account, which resulted in higher final pH values. Prior to isotopic analysis, samples were thawed and mixed well. Ammonium concentrations were determined at the University of Southern California (USC, USA), and the results were compared to the shipboard measurements in order to assure the adequate preservation of ammonium in the samples. The USC analyses and the shipboard analyses for Site 1227 agree within 2%. However, USC analyses of samples from Site 1230 are consistently lower than shipboard measurements by 10%. The amount of N collected on acidified filters during our ammonium extraction procedure (see below) and measured as a peak area on the mass spectrometer agrees within 2% with expected amount of N based on concentrations obtained at USC. Therefore, we conclude that the 10% difference between USC and shipboard analyses stems from discrepancies in the calibrations. The loss of ammonium during storage is unlikely because such loss would also have caused considerable scatter in $\delta^{15}N$, which was not observed.

Ammonium was extracted on acidified glass fiber filters using a method of Sorensen and Jensen (1991), Sigman et al. (1997), and Holmes et al. (1998). In brief, diluted pore water was placed in polypropylene centrifuge tubes, and pH was adjusted to >10 by addition of finely ground MgO, precombusted at 450°C. This converted NH_4^+ to uncharged NH_3. A "trap" made of a Teflon tape envelope containing a glass fiber filter grade C or glass fiber filter grade F wetted with 20 µL of 2-M H_2SO_4 was then added to each tube. The uncharged NH_3 diffused through the Teflon membrane was protonated inside the "trap" and collected on the filter.

Nitrogen isotopic ratios of sediments and of ammonium trapped on the filters were measured at USC on an Isoprime Micromass mass spectrometer, interfaced with a Carlo Erba CHN-2500 elemental analyzer in the continuous flow mode. Isotopic ratios were determined against a reference N_2 (ultra high purity grade, Gilmore) that has been calibrated against a set of National Institute of Standards and Technology (NIST) standards, IAEA N1 and IAEA N2, routinely run in the USC stable isotope laboratory. NIST standards were run daily as internal standards. The daily precision, based on the internal standards, was 0.2‰ or better. Procedural standards of known isotopic composition, similar in concentration and volume to samples, were prepared and carried through the whole extraction procedure with each set of samples. The sample standard deviation based on replicate analyses of both samples and standards was typically 0.50‰. The $\delta^{15}N$ of procedural standards of ammonium was usually ~0.5‰ lighter than expected, likely due to either a procedural artifact or perhaps a small reagent blank. The amount of nitrogen in standards was always close to that in samples, so $\delta^{15}N$ values of samples were corrected by adding 0.5‰ to the measured values. Typical size of the nitrogen blank was 0.2 to 0.3 µmol, while samples contained 6–7 µmol of N. Extraction efficiencies (yields) varied ranged between 97% and 103% for both sets of samples.

SITE 1230

Site Description and Lithology

Site 1230 is located on the lower slope of the Peru Trench (9°6.7525′S, 80°35.0100′W) within 100 m of the location of ODP Leg 112 Site 685 (Fig. F1). Water depth at this site is 5086 m, but biogeochemical processes observed in the sediments are more typical of an ocean margin than a deep-sea setting (D'Hondt, Jørgensen, Miller, et al., 2003; Suess, von Huene, et al., 1988). The sediments at Site 1230 were divided into two lithostratigraphic units. Unit I (0–215.8 meters below seafloor [mbsf]) is Holocene–Pleistocene in age and consists of biogenic sediments mixed with siliciclastic components (D'Hondt, Jørgensen, Miller, et al., 2003). The sequence is characterized by alternating layers of diatom-nannofossil ooze and marl with dark gray to olive clays. Graded layers were presumably deposited by turbidite events that originated most likely near the shelf break and incorporated material from intermediate depths along the way (Suess, von Huene, et al., 1988). Unit II (215.8–278.3 mbsf) was deposited during the Miocene and is separated from Unit I by an unconformity. The presence of a fractured layer at this horizon suggests the unconformity is of tectonic origin. Sediments consist of diatom- and silt-rich deposits interbedded with clay rich layers. Estimated sediment accumulation rates for Quaternary

F1. Map of locations, p. 18.

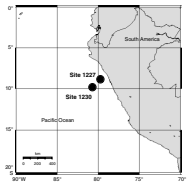

and Miocene sequences are 100 m/m.y. and 200 m/m.y., respectively (Suess, von Huene, et al., 1988).

Results

Biogeochemistry of Pore Water

Concentrations of both dissolved inorganic carbon (DIC) and ammonium, the major metabolites of microbial decomposition of organic matter, are exceptionally high at this site. Concentrations of DIC reach a maximum of 162 mM at 132 mbsf, decreasing to ~130 mM below 200 mbsf. Ammonium concentrations reach a maximum value of 38 mM at about the same depth as the DIC maximum; similar to DIC concentrations, they decrease below 132 mbsf to ~25 mM at the bottom of the measured profile at 250 mbsf (D'Hondt, Jørgensen, Miller, et al., 2003).

Sulfate is depleted below the detection limit within the upper 7 mbsf, and dissolved methane concentrations increase steeply below this horizon, reaching values up to 7 mM at 17 mbsf. The sediments at this site also contain methane hydrates (Suess, von Huene, et al., 1988; D'Hondt, Jørgensen, Miller, et al., 2003).

Solid-Phase Composition; $\delta^{15}N$ of Pore Water Ammonium and Sedimentary Organic Matter

TOC concentrations at Site 1230 have moderate values of ~2 wt% (TOC measurements, details, and results are presented in **Meister et al.,** this volume), and TN ranges between 0.3 and 0.4 wt% (Fig. **F2**). Calculations using experimentally derived values for ammonium distribution coefficient (Prokopenko, 2004) indicate that adsorbed ammonium constitutes no more than 10% of TN values (the values vary with porosity and pore water ammonium concentrations). Atomic C/N ratios are between 9 and 11 and are relatively constant through the whole sediment column (Table **T1**). Nitrogen isotopic ratios of the sediments vary between 5‰ and 7.5‰ (average value = 5.71‰ ± 0.19‰) and do not show any significant change with depth (Fig. **F3**). Three horizons at 47, 72, and 100 mbsf have higher $\delta^{15}N$ values of 7.5‰–8‰.

The isotopic composition of ammonium is relatively constant through the whole profile, with most values between 4.6‰ and 5.9‰ (Fig. **F2**). The average $\delta^{15}N$ of pore water ammonium at this site is 5.0‰ ± 0.1‰, which is ~0.7‰ ± 0.2‰ lighter than the average $\delta^{15}N$ of sediments.

Discussion

Diagenesis and Nitrogen Isotopic Composition of Pore Water Ammonium and Sedimentary Organic Nitrogen

The ammonium and DIC profiles indicate that the labile organic matter in Unit I is decomposed as it is buried, releasing both metabolites. The maximum DIC and ammonium concentrations create downward diffusion into Unit II, which apparently had lower solute concentrations of both metabolites before its tectonic juxtaposition with Unit I. Both units have organic matter with similar $\delta^{15}N$, so diffusion of ammonium across the unconformity should not strongly influence the $\delta^{15}N$ of ammonium. Indeed, our measurements showed no change in $\delta^{15}N$ of pore water ammonium across the boundary.

F2. TOC and TN, Site 1230, p. 19.

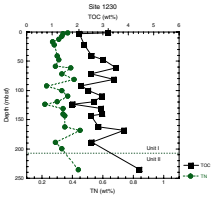

T1. Sediment composition, Hole 1230A, p. 28.

F3. Ammonium and $\delta^{15}N$ of ammonium and bulk sediments, Site 1230, p. 20.

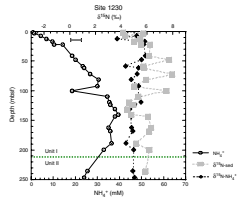

Because ammonium is the product of the organic matter decomposition, we can calculate the amount of organic nitrogen (N_{org}) lost to degradation as a function of depth based on the amount of ammonium released through a sediment interval. The approach is based on flux calculations at the upper and lower boundaries of Unit I and estimates nitrogen loss for all of Unit I. In this approach, we determined tangents to the ammonium profile near the top (1.35 mbsf) of the sediment column and near the ammonium maximum (119.47 mbsf). We used these tangents to calculate diffusive fluxes based on Fick's first law. The advective contribution to the total ammonium flux was deemed unimportant (Peclet number = 3) (Table T2). Therefore, advective flux was not included in the calculations. The calculated difference of 0.98 ± 0.20 µmol/(cm²yr) represents the net nitrogen released from solid phases through this interval. The present sedimentation flux of organic nitrogen was calculated using the average sediment accumulation rate of 100 m/m.y. (D'Hondt, Jørgensen, Miller, et al., 2003), average porosity of 0.75, and nitrogen in the topmost interval of 0.37 wt%. The N_{org} sedimentation flux at 1.35 mbsf is 1.59 ± 0.30 µmol/(cm²yr). Thus, the ammonium production flux indicates that ~60% ± 15% of N_{org} being deposited at 1.35 mbsf is decomposed and lost as ammonium. However, it is likely that flux at the 119.47-mbsf horizon is not quite in a steady state due to currently occurring diffusion of ammonium into the Layer II of Miocene age. Consequently, 60% loss of N_{org} via decomposition may be just a minimum estimate of the amount of N_{org} lost. The average isotopic composition of ammonium is 0.7‰ ± 0.2‰ lighter than the $\delta^{15}N$ of N_{org}. One possible explanation for this difference may be a small contribution from dissolved organic nitrogen (DON) in the pore water, if it degraded during the ammonium extraction procedure (Sigman, 1997). Dissolved organic carbon (DOC) at this site reaches concentrations of 20 mM (**Smith,** this volume). DON concentrations were not measured during Leg 201, but the contribution from DON is probably minor (D. Smith, pers. comm., 2004).

Another possibility is that the difference is a result of fractionation associated with release of ammonium from decomposing organic matter with a fractionation factor, ε = –0.7‰ ± 0.2‰. Despite the fact that at least half of organic nitrogen has been lost to diagenesis between 1.35 and 119.47 mbsf, there is no pronounced change in the isotopic composition of the sediments with depth. If the small isotopic enrichment of ammonium is indeed due to fractionation during ammonium release, the expected change in the solid-phase $\delta^{15}N$ would have been negligibly small, ~0.7‰. The absence of depth dependency of $\delta^{15}N$ of the sedimentary nitrogen and close similarity between $\delta^{15}N$ of ammonium solid-phase N both suggest that at Site 1230 little isotopic fractionation is associated with long-term diagenesis of sedimentary organic matter. One additional implication is that the $\delta^{15}N$ of material reaching the sediments at this site has been rather constant through time.

T2. Parameters for modeling results, Sites 1230 and 1227, p. 29.

SITE 1227

Site Description and Lithology

Site 1227 is located on the Peru margin at 8°59.46'S, 79°57.34'W, ~100 m from the location of ODP Leg 112 Site 684 in the Trujillo Basin, which is a small, fault-bounded pond of sediments. Water depth at this

location is 427.5 m. Presently, this site is positioned within the upwelling system. The sediment succession consists of four lithologically distinct units and contains a mixture of marine and terrestrial components (Suess, von Huene, et al., 1988; D'Hondt, Jørgensen, Miller, et al., 2003).

The age of Unit I sediments (0–11.95 mbsf) is <0.9 Ma. They are mostly laminated and consist of diatom-bearing silt and clay-rich diatom ooze with occasional foraminiferal ooze layers. Unit I was deposited under a strong upwelling regime. Unit II (11.1–34.1 mbsf), of Pleistocene age, contains dark olive, bioturbated, silty sediments with glauconite and phosphate layers that indicate possible winnowing of sediments during the times of sea level lowstand (Suess, von Huene, et al., 1988). Variations in the amount of terrigenous input for Unit II and evidence for sediment winnowing by bottom currents are attributed to fluctuations in sea level throughout the depositional history of Unit II. Unit III (34.1–53.1 mbsf), of Pliocene age (Suess, von Huene, et al., 1988), is characterized by reduced diatom abundance and a high percentage of clay, feldspar, and quartz, which implies the presence of higher terrigenous input in this unit. Vertically graded sequences are common. Overall, the unit exhibits a fining-upward trend; sediments are bioturbated. A strong porosity minimum, accompanied by grain density and magnetic susceptibility maxima, is observed in the interval between 40 and 50 mbsf. Unit IV (53.1–151 mbsf), of late Miocene age, is separated from the overlying Unit III by a large unconformity; its duration spans 5.7–8.7 Ma (Suess, von Huene, et al., 1988). The sediments of Unit IV are mostly dark green clays and nannofossil-bearing ooze. Volcanic ash layers and volcanic shards occur through the unit. Laminated dolomite layers are present. Overall, this unit is characterized by a lower terrigenous input than the three stratigraphic units above it. It was also least affected by bioturbation and reworking by currents. Estimated sediment accumulation rates are 20 m/m.y. for the Quaternary sequence, 30 m/m.y. for the Pliocene, and 50 m/m.y. for the Miocene (Suess, von Huene, et al., 1988).

Results

Biogeochemistry of Pore Water

The concentrations of major metabolites and electron acceptors in the pore fluids of Site 1227 indicate the presence of active microbial communities in these sediments (D'Hondt, Jørgensen, Miller, et al., 2003). Sulfate concentrations decrease downcore from seawater values to below the detection limit at ~40 mbsf (Fig. F4). Methane concentrations increase steeply below 38 mbsf.

DIC concentrations reach a maximum of ~25 mM at 38 mbsf, in the sulfate–methane transition zone. Below this horizon, DIC decreases to 20 mM and concentrations remain constant through the rest of the sediment column recovered. Concentrations of pore water ammonium increase steadily with depth (Fig. F5), reaching 23 mM at the bottom of the profile. At the boundary between Units II and III (36–38 mbsf), the gradient of ammonium concentrations shows a pronounced kink in data from Hole 1227A, with a steep gradient in Unit III below a smaller gradient in Unit II. Results from Hole 1227D do not indicate a distinct kink but have lower sampling resolution. Core recovery in the interval between 43 and 72 mbsf was poor (D'Hondt, Jørgensen, Miller, et al., 2003), which might have led to contamination of some samples with

F4. Pore water sulfate, Site 1227, p. 21.

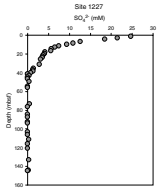

F5. Ammonium and $\delta^{15}N$ of ammonium and bulk sediments, Site 1227, p. 22.

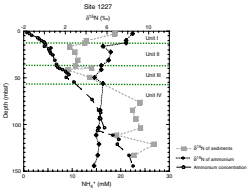

seawater. However, sulfate concentrations (Fig. F4) show little evidence of such contamination, clearly <5%. The ammonium profile obtained during Leg 112 (Suess, von Huene, et al., 1988) also exhibits a change in the gradient at the same depth horizon. In contrast to ammonium, chloride concentrations increase steadily with depth, with no significant kinks in the profile (Fig. F6). The location of the kink coincides with the interval of sulfate–methane transition. Sediments of Unit III, just below the kink, have lower porosity than in adjacent horizons.

F6. Pore water chloride and ammonium, Site 1227, p. 23.

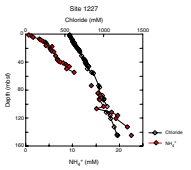

F7. TOC and TN, Site 1227, p. 24.

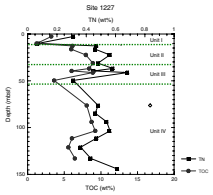

T3. Sediment composition, Hole 1227A, p. 30.

Elemental and Nitrogen Isotope Composition of Sedimentary Organic Matter and Pore Water Ammonium

Sediments from Site 1227 are rich in organic matter, which is typical for highly productive upwelling regions (Fig. F7; Table T3). Concentrations of organic carbon are 5–9 wt% and total nitrogen 0.4–0.6 wt%. Adsorbed ammonium constitutes 1%–10% of TN (calculated as discussed for Site 1230). Atomic C/N ratios vary between 12 and 21. Relatively high values of sedimentary C/N ratios are consistent with episodic input of terrestrial organic matter, suggested by the sedimentological evidence. The overall trend of C/N increasing with depth through the upper 35m may indicate possible preferential remineralization of N-containing compounds.

Sedimentary $\delta^{15}N$ values for these lithologic units vary (Fig. F7; Table T3). Nitrogen isotope ratios in Unit I (last 0.9 m.y.) change from 6.8‰ to 4‰ downcore. Sediments of Units II and III (Pliocene) have $\delta^{15}N$ values between 2‰ and 4‰. Unit IV (Miocene sediments) is characterized by significantly heavier isotopic values, at ~9‰–10‰.

Nitrogen isotope ratios of pore water ammonium show a different pattern (Fig. F7; Table T3) and far less variation than solid phases. Ammonium $\delta^{15}N$ is 3‰–4‰ heavier than sedimentary $\delta^{15}N$ in the upper 36 mbsf (Units I and II) and becomes progressively lighter from ~8‰ near the sediment/water interface to ~5‰ at 36 mbsf. The isotopic composition of ammonium in pore water of Units III and IV is lighter than sedimentary $\delta^{15}N$ and decreases from 5‰ in Unit III and the upper part of Unit IV to ~4.5‰ downcore. In Unit III, the ammonium isotopic composition is fairly close to the sedimentary $\delta^{15}N$; in Unit IV, ammonium is ~5‰, which is 4‰ lighter than the sedimentary $\delta^{15}N$ (Fig. F7).

Discussion

Sources and Sinks of Pore Water Ammonium

Pore water biogeochemistry and the structure of ammonium concentration and isotopic composition at Site 1227 are very complex. Increasing concentrations of pore water ammonium downcore usually indicate continuous degradation of organic matter at depth. However, at Site 1227, the pore water chemistry is influenced by the presence of a hypersaline subsurface brine of Miocene age below 40–50 mbsf (Suess, von Huene, et al., 1988), as manifested by increasing concentrations of Mg^{2+}, Ca^{2+}, Na^+, and Cl^- with depth (Suess, von Huene, et al., 1988; D'Hondt, Jørgensen, Miller, et al., 2003).

A nearly linear relationship between NH_4^+ and Cl^- concentrations (Fig. F8) below 36.95 mbsf suggests that the predominant source of am-

F8. Pore water ammonium vs. chloride, Site 1227, p. 25.

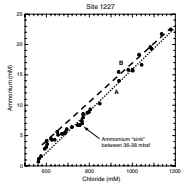

monium diffusing toward this horizon is the brine, rather than decomposing organic matter. Above the 36.95-mbsf depth horizon, ammonium is probably added by decomposition of organic matter, as indicated by concave-down shape of the plot for the upper interval. The kink in the ammonia profile near 37 mbsf shows up on Figure **F8** as a local minimum. Undoubtedly, the kink is partially attributable to the relatively low porosity layer near the top of Unit III, which should require a steeper gradient for ammonium to balance fluxes. However, the gradient for chloride should also steepen, and Figure **F8** should indicate linearity through this region if both solutes behave conservatively and the system is in steady state. As noted above, sulfate shows little indication that the samples were significantly diluted with seawater during recovery, and the good agreement of shipboard and USC ammonium measurements is evidence that the kink is not a result of analytical problems. If the system is in steady state, Figure **F8** is strong evidence that the kink reflects a local sink for ammonium, separating deep sources (predominantly the brine) and shallower sources from decomposing organic matter.

The localization of sink near this horizon might be reasonable, as it lies in the sulfate–methane transition horizon, where pH changes occur and new mineral phases, such as carbonates, are likely to precipitate (**Meister et al.,** this volume). Struvite ($MgNH_4PO_4$) could be a candidate phase (Elderfield et al., 1981). Laboratory experiments demonstrated coprecipitation of struvite with Mg-bearing carbonate minerals (Pontoizeau et al., 1996; Rivadeneyra et al., 2006). But degree of struvite saturation at the ambient pH of ~7 in these pore waters is <0.001. Consequently, it is unclear what phase might provide a sink in this horizon.

Nitrogen isotopes provide some additional insights into the nature of sources and sinks that must exist. A useful approach is to construct a mixing diagram, where $\delta^{15}N$ of ammonium is plotted against inverse concentrations, $[NH_4^+]^{-1}$ (Fig. **F9**), as described by Faure and Mensing (2005). On such diagram, conservative mixing between two localized ammonium sources with different isotopic compositions and concentrations would result in a straight line connecting the $\delta^{15}N$ values of the end-members, if the profile is in a steady state. Deviations from a linear relationship indicate additional sources or sinks through the region sampled. The shape of the curvature depends on the isotopic composition of the nitrogen added (or lost) and the depth region in which it is added. If diffusion is the dominant transport mechanism and steady state exists, a tangent to the data points, extrapolated to the y-intercept, indicates the composition of the net upward ammonium flux.

From the mixing diagram (Fig. **F9**), we can identify four features that correlate with the sources and sink identified based on the concentration profiles and the ammonium vs. chloride. Three sources are associated with different lithologic units: (1) ammonium in Unit IV diffusing upward from the brine with $\delta^{15}N$ of ~4.4‰ as indicated by projected intercept, (2) ammonium with isotopic composition of ~8‰ added through the Units I and II, and (3) a small and not readily apparent ammonium source in Unit III that adds $\delta^{15}N$ of ~6‰. Finally, the sink in the kink region alters the relationship so that the extrapolated tangent indicates the upward flux has become isotopically lighter. This requires that the sink preferentially removes ^{15}N. In addition, ammonium is lost at the sediment/water interface.

In Unit IV, the nearly linear trend formed by the data points indicates predominantly conservative mixing between ammonium diffus-

F9. Mixing diagram, Site 1227, p. 26.

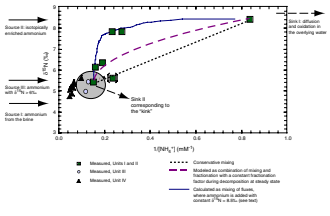

ing from the brine and ammonium released in Unit III (Fig. F9). The data from Units I and II, on the other hand, strongly deviate from the simple mixing relationship illustrated by the dotted line in Figure F9. The steady-state interpretation requires continuous production of heavier ammonium along the mixing path. The region inside the gray circle is strongly influenced by the sink near 37 mbsf, which affects isotopic composition as well as concentration.

The isotopic composition of the required sources and the sink can be estimated by calculating mass balances. A two-layer reaction-diffusion model (for $^{14}NH_4^+$ and $^{15}NH_4^+$) was constructed with the assumption of a steady-state condition (detailed description of formulations used in this model is given in Prokopenko et al. [2006]) and applied to calculate diffusive ammonium fluxes toward and away from the 36.95-mbsf horizon. Isotopic composition of the fluxes was calculated as follows:

$$\delta^{15}N_{flux} = [(^{15}J/^{14}J)/R_{std} - 1) \times 1000,$$

where J is the flux of $^{15}NH_4^+$ and $^{14}NH_4^+$, respectively, R_{std} is $^{15}N/^{14}N$ ratio in the atmospheric N_2 gas. Advective transport was ignored, as the Peclet number is >>1 (Table T2). Fluxes were calculated as first derivatives of the concentrations according to Fick's first law. Flux leaving Unit III, just below the 36.95-mbsf horizon, is 0.56 ± 0.20 µmol/(cm²yr) with isotopic composition of 5.8‰, while the upward flux from this horizon is 0.14 ± 0.05 µmol/(cm²yr) with $\delta^{15}N$ of 0.9‰ (see Fig. F10). Therefore, our calculations show that ~75% of ammonium may be lost in the vicinity of the 36.95-mbsf horizon, if the ammonium profile is currently in the steady state. The loss is accompanied by small positive isotopic fractionation with the fractionation factor of approximately +3.0‰ ± 0.5‰. This small positive isotopic fractionation associated with the apparent sink would point toward a nonbiological mechanism, as biological ammonium uptake is usually accompanied by large-magnitude negative isotopic fractionation (Hoch et al., 1992).

The interpretation of the ammonium sources, as well as the sinks suggested by the changes of slopes on the mixing diagram, strongly depends on whether the represented system in the steady-state condition. We limit the following discussion to the upper 40 mbsf (Units I and II), since below this horizon the major source of ammonium is the Miocene brine, and factors controlling its $\delta^{15}N$ are presently unknown.

F10. Ammonium fluxes and $\delta^{15}N$ of the fluxes, Site 1227, p. 27.

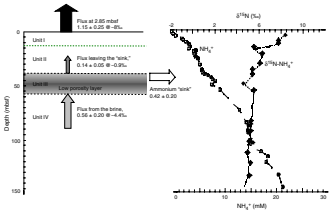

Nitrogen Budget at Steady State in Units I and II

Assuming a steady-state condition and applying the reaction-diffusion model (Prokopenko, 2004), we calculated the magnitude of the ammonium fluxes at several depth horizons through the upper 37 mbsf of the sediments and relative contribution of the ammonium flux from below (0.14 µmol/[cm²yr]) to the total flux at each of these horizons. Then, $\delta^{15}N$ of total ammonium at each horizon was calculated as the isotopic mass balance between the $\delta^{15}N$ of flux from below 36.95-mbsf horizon (5.5‰, observed) and a heavier ammonium with constant isotopic composition added through Units I and II. The best fit to the data points was obtained with $\delta^{15}N$ of the heavier end-member of 8.5 (Fig. F9, solid line).

The average isotopic composition of the bulk sedimentary nitrogen in the upper 36.95 mbsf of the sediments is 3.8‰. This is ~4.7‰ lighter than the $\delta^{15}N$ of 8.5‰ of ammonium flux added to the pore wa-

ter through this interval. So, the question relevant to the present study is what is the mechanism of the apparent isotopic enrichment of pore water ammonium relative to the organic nitrogen in the upper 36 mbsf of the sediments at Site 1227?

If the ammonium concentration and $\delta^{15}N$ profiles are in steady state, then the enrichment of ammonium in heavier isotopes relative to N_{org} signifies a loss of the isotopically heavier nitrogen from organic matter through Units I and II. In this case, as diagenesis progresses, the preserved organic matter should become isotopically lighter. Indeed, measured $\delta^{15}N$ of sedimentary organic nitrogen in Units I and II (Fig. F6) becomes progressively lighter downcore, changing from 6.8‰ at the surface to ~4‰ in the lower part of Unit I, and reaching values between 2.5‰ and 3‰ within Unit II. Consequently, if the ammonium profile at Site 1227 is in steady state, diagenetic processes at this site result in the $\delta^{15}N$ shift of ~4‰ in preserved organic nitrogen. Isotopically heavier ammonium might be released via one of the following mechanisms: (1) preferential degradation of isotopically heavier organic N (Macko and Estep, 1984), that might be more labile; (2) preferential assimilation of isotopically lighter ammonium into bacterial biomass (Lehmann et al., 2002); or (3) preferential decomposition of an isotopically heavier, more labile marine fraction of organic matter relative to a more refractory terrestrial component (Prokopenko et al., 2006; Sweeney and Kaplan, 1980). High C/N ratios in the sediments of Site 1227 imply that significant component of terrestrial organic matter is present, although the sediment supply may come from settings that are currently relatively arid. The $\delta^{15}N$ of the isotopically heavier ammonium end-member of 8.5‰ is consistent with the marine origin of the source organic matter. Therefore, the latter scenario could be responsible for the observed isotopic enrichment of pore water ammonium relative to the sedimentary nitrogen, if the system is in steady state.

The steady-state reaction-diffusion model of Prokopenko (2004) was used to predict the $\delta^{15}N$ of pore water ammonium, which would result from mixing between the brine source and ammonium contributed from decomposition of organic matter occurring with the fractionation factor of 2‰. The $\delta^{15}N$ of ammonium released at 2.85 mbsf (our shallowest data point and a "zero" depth in the model) was set to be 8.5‰. The results are plotted on the mixing diagram as a dashed line and indicate that while this process does cause a deviation from the conservative mixing relationship, it cannot fully account for the observed enrichment of pore water ammonium relative to the N_{org}.

Finally, we calculated the ammonium production in the interval between 2.85 and 36.96 mbsf. Applying the approach described for Site 1230, we find that present-day ammonium flux produced throughout this interval cannot be supported by the sedimentation flux of N_{org} with the N concentration equal to the topmost measured interval concentration, which is 0.31 wt%. The ammonium production flux is ~1.1 ± 0.15 μmol/(cm²yr), while N_{org} accumulation flux at 2.85 mbsf is 0.22 ± 0.05 μmol/(cm²yr) (calculated from average porosity 0.8 and concentration of N = 0.31 wt%). The unsupported ammonium flux, most likely, results from the variability of the weight percent of organic nitrogen through time, or, in other words, the nonsteady-state depositional history of the sediments at Site 1227.

Evaluating our assumption of the steady-state condition at Site 1227, we conclude that the steady-state scenario leaves two problems unresolved: (1) our estimated ammonium production flux exceeds our esti-

mate of the organic N burial flux at 2.85 mbsf, and (2) the isotopic composition of ammonium predicted by our steady-state model substantially deviates from the observed data (Fig. F9).

Nonsteady-State Scenario

An alternative scenario is that the ammonium profile and its isotopic composition represents a nonsteady-state condition, where $\delta^{15}N$ of ammonium is strongly affected by the contribution from the decomposition of recently deposited organic matter with $\delta^{15}N > 8‰$. If a pulse of organic-rich material with the heavier $\delta^{15}N$ has been deposited within the last several thousand years, under the regime of intense postglacial upwelling, a corresponding pulse of isotopically enriched ammonium should be released into the pore water. This would create an isotopically distinct diffusive front that would propagate downward.

At present, the isotopically heavier ammonium from the pulse of organic matter deposited during the last 10 k.y. would have influence to a depth of ~30 mbsf if

$$\bar{\chi} = 2\sqrt{D_s t},$$

where

$\bar{\chi}$ = mean distance of diffusion,
D_s = 8.12×10^{-6} cm²/s is the diffusion coefficient of ammonium in the sediments with porosity = 0.8, and
t = time.

In this case, the isotopic enrichment of pore water $\delta^{15}N$ relative to $\delta^{15}N$ of N_{org} would be due to the addition of the new, isotopically heavier endmember rather than fractionation during the decomposition of organic matter.

With an average sedimentation rate of 20 m/m.y. estimated for Site 1227, the upper 2 m of the sediment column would represent ~100 k.y. Our first isotopic measurement was done at a depth of 2.85 mbsf, so $\delta^{15}N$ of the modern surface sediments is unknown. In a region ~2° south of Site 1227, the reported isotopic composition of modern organic matter is between 6‰ and 8‰ (Libes and Deuser, 1988). At a site ~4° south of Site 1227, Ganeshram et al. (2000) reported sedimentary values of $\delta^{15}N$ for the last 100 k.y. that vary between 6‰ and 11‰. From those studies, we can infer the values of $\delta^{15}N$ of the organic matter deposited in this region to be most likely between 8‰ and 10‰. In this case, isotopic composition of ammonium through the upper 36.95 mbsf of the sediment column at Site 1227 may be dominated by mixing between ammonium of 8‰–10‰ released in the upper 1–2 mbsf and ammonium coming from the brine (with isotopic composition of ~5‰). If this recently deposited material had higher reactivity than the older material, it could have a pronounced effect on the mass balance for both ammonium and its $\delta^{15}N$.

The nonsteady-state hypothesis would offer an alternative explanation for the change in the concentration gradient at 37 mbsf. It seems possible that the apparent coincidence of the methane/sulfate boundary and the diffusing ammonium pulse both represent the influence of the low porosity zone, which would retard downward transport of both sulfate and the nonsteady-state pulse of recently added ammonium.

Further measurements of near-surface sediments are required test this hypothesis. Finally, a nonsteady-state influence on ammonium behavior would not preclude application of steady-state models to other pore water solutes because the response time would depend on the length scale of the solute in question. Sulfate, for example, has a much shorter length scale and should have reached nearly steady-state distribution during the past 10 k.y.

SUMMARY

Our results from Site 1230 indicate that the isotopic composition of pore water ammonium differs from the $\delta^{15}N$ of sedimentary organic matter by <1‰, pointing toward absence of significant isotopic fractionation during organic matter diagenesis. At this site, the sedimentary organic matter is of predominantly marine origin, as suggested by atomic C/N ratios of 9–11. These findings confirm the hypothesis put forth by Altabet et al. (1999), who postulated that in rapidly accumulating organic-rich coastal sediments, organic matter decomposes without significant isotopic fractionation. A similar conclusion was reached based on the results obtained from the sediments collected at Sites 1234 and 1235 along the Chile margin during the ODP Leg 202 (Prokopenko et al., in press), where no or little isotopic fractionation between N_{org} and pore water ammonium was observed. In those sediments, the sedimentary organic matter was found to be of marine origin as well. All three sites were characterized by rapid sediment accumulation rates, so that the sedimentary columns represent 150–200 k.y. of depositional history. The constant (±1‰) $\delta^{15}N$ of sedimentary N_{org} through depth at these sites indicates little variation in the isotopic composition of organic matter deposited during this time interval.

At Site 1227, the interpretation of the $\delta^{15}N$ of ammonium profile is complicated by several factors: addition of isotopically different ammonium from the brine and variability in concentrations and isotopic composition of deposited organic matter through time, which possibly led to a nonsteady-state condition of the current ammonium profile.

If the ammonium profile at Site 1227 is in steady state, then an effective fractionation of ~4‰ exists between decomposing organic matter and released ammonium, most likely due to preferential decomposition of the marine fraction of sedimentary organic matter that contains both marine and terrestrial components, as suggested by Sweeney and Kaplan (1980).

However, it appears that at Site 1227 several factors have varied through time. These factors include the weight percent of N, its lability, and its isotopic composition. If these changes have occurred in the recent past, the present profile of ammonium concentrations and its $\delta^{15}N$ might have not reached a new steady state. The time-dependent variation in $\delta^{15}N$ of the organic matter deposited on the ocean floor would result in a mixing pattern between ammonium released in the upper few meters of the sediment column and ammonium diffusing from below. The mixing between two end-members with different isotopic compositions would lead to the apparent isotopic enrichment of ammonium relative to the organic matter at depth.

Synthesizing results from Sites 1227 and 1230, we can conclude that no significant fractionation is associated with diagenesis of marine organic matter deposited at the ocean margins, such as at Site 1230. When a significant fraction of a terrestrial component is

present, preferential decomposition of the marine fraction, which is usually enriched in ^{15}N isotopes relative to terrestrial organic matter may lead to an overall decrease in $\delta^{15}N$ of bulk sediments downcore. However, further work in a less complex system than Site 1227 is required to confirm this conclusion.

ACKNOWLEDGMENTS

This research used samples and/or data provided by the Ocean Drilling Program (ODP). ODP is sponsored by U.S. National Science Foundation (NSF) and participating countries under management of Joint Oceanographic Institutions (JOI), Inc. This study was supported by NSF grant OCE-0136500 to D.H. and an ODP Schlanger fellowship to M.G.P. The authors gratefully acknowledge members of the Scientific Party of Leg 201, who collected samples for us. We also extend our gratitude to the Co-Chief Scientists of Leg 201, Drs. S. D'Hondt and B.B. Jørgensen for being very helpful in obtaining the samples, and thus making this study possible. The technical assistance of M. Rincon and T. Gunderson at USC is greatly appreciated. The thoughtful reviews of three anonymous reviewers and S. D'Hondt improved this manuscript significantly.

REFERENCES

Altabet, M.A., Deuser, W.G., Honjo, and S., Steinen, C., 1991. Seasonal and depth-related changes in the source of sinking particles in the North Atlantic. *Nature, (London, U. K.),* 354(6349):136–139. **doi:10.1038/354136a0**

Altabet, M.A., and Francois, R., 1994. Sedimentary nitrogen isotopic ratio as a record for surface ocean nitrate utilization. *Global Biogeochem. Cycles,* 8(1):103–116. **doi:10.1029/93GB03396**

Altabet, M.A., and McCarthy, J.J., 1985. Temporal and spatial variations in the natural abundance of ^{15}N in PON from a warm-core ring. *Deep-Sea Res. Part A,* 32(7):755–772. **doi:10.1016/0198-0149(85)90113-X**

Altabet, M.A., Pilskaln, C., Thunell, R. and Pride, C., Sigman, D., Chavez, F., and Francois, R., 1999. The nitrogen isotope biogeochemistry of sinking particles from the margin of the eastern North Pacific. *Deep-Sea Research I,* 46(4):655–679. **doi:10.1016/S0967-0637(98)00084-3**

Berger, W.H., and Keir, R.S., 1984. Glacial–Holocene changes in atmospheric CO_2 and the deep-sea record. *In* Hansen, J.E., and Takahashi, T. (Eds.), *Climate Processes and Climate Sensitivity.* Maurice Ewing Ser., 29:337–351.

Berner, R.A., 1980. *Early Diagenesis: A Theoretical Approach:* Princeton, NJ (Princeton Univ. Press).

Boudreau, B.P., 1997. *Diagenetic Models and Their Implementation: Modeling Transport and Reaction in the Aquatic Sediments:* Berlin (Springer Verlag).

Broecker, W.S., 1982. Glacial to interglacial changes in ocean chemistry. *Prog. Oceanogr.,* 11:151–197. **doi:10.1016/0079-6611(82)90007-6**

D'Hondt, S.L., Jørgensen, B.B., Miller, D.J., et al., 2003. *Proc. ODP, Init. Repts.,* 201 [CD-ROM]. Available from: Ocean Drilling Program, Texas A&M University, College Station TX 77845-9547, USA. [**HTML**]

Elderfield, H., McCaffrey, R.J.H., Luedtke, N., Bender, M., and Truesdale, V.W., 1981. Chemical diagenesis in Narragansett Bay sediments. *Am. J. Sci.,* 281:1021–1055.

Falkowski, P.G., 1997. Evolution of the nitrogen cycle and its influence on the biological sequestration of CO_2 in the ocean. *Nature (London, U. K.),* 387(6630):272–275. **doi:10.1038/387272a0**

Faure, G., and Mensing, T.M., 2005. *Isotopes: Principles and Applications:* New Jersey (John Wiley & Sons).

Francois, R., Altabet, M.A., and Burckle, L.H., 1992. Glacial to interglacial changes in surface nitrate utilization in the Indian sector of the Southern Ocean as recorded by sediment $\delta^{15}N$. *Paleoceanography,* 7:589–606.

Ganeshram, R.S., Pedersen, T.F., Calvert, S.E., McNeill, G.W., and, Fontugne, M.R., 2000. Glacial-interglacial variability in denitrification in the world's oceans: causes and consequences. *Paleoceanography,* 15(4):361–376. **doi:10.1029/1999PA000422**

Ganeshram, R.S., Pedersen, T.F., Calvert, S.E., and Murray, J.W., 1995. Large changes in oceanic nutrient inventories from glacial to interglacial periods. *Nature (London, U. K.),* 376(6543):755–758. **doi:10.1038/376755a0**

Gruber, N., 2004. The dynamics of the marine nitrogen cycle and its influence on atmospheric CO_2. *In* Follows, M., and Oguz, T. (Eds), *The Ocean Carbon Cycle and Climate.* NATO ASI Ser., 97–148.

Haug, G.H., Pedersen, T.F., Sigman, D.M., Calvert, S.E., Nielsen, B., and Peterson, L.C., 1998. Glacial/interglacial variations in production and nitrogen fixation in the Cariaco Basin during the last 580 kyr. *Paleoceanography,* 13(5):427–432. **doi:10.1029/98PA01976**

Hoch, M.P., Fogel, M.L. and Kirchman, D.L., 1992. Isotope fractionation associated with ammonium uptake by a marine bacterium. *Limnol. Oceanogr.,* 37(7):1447–1459.

Holmes, R.M., McClelland, J.W., Sigman, D.M., Fry, B. and Peterson, B.J., 1998. Measuring N-15-NH_4^+ in marine, estuarine and fresh waters: an adaptation of the

ammonia diffusion method for samples with low ammonium concentrations. *Mar. Chem.,* 60(3-4):235–243. **doi:10.1016/S0304-4203(97)00099-6**

Lehmann, M.F., Bernasconi, S.M., Barbieri, A. and McKenzie, J.A., 2002. Preservation of organic matter and alteration of its carbon and nitrogen isotope composition during simulated and in situ early sedimentary diagenesis. *Geochim. Cosmochim. Acta,* 66(20):3573-3584. **doi:10.1016/S0016-7037(02)00968-7**

Li, Y.-H., and Gregory, S., 1974. Diffusion of ions in seawater and deep sea sediments. *Geochim. Cosmochim. Acta,* 38:703–714.

Libes, S.M., and Deuser, W.G., 1988. The isotope geochemistry of particulate nitrogen in the Peru Upwelling Area and the Gulf of Maine. *Deep-Sea Res. Part A,* 35(4):517–533. **doi:10.1016/0198-0149(88)90129-X**

Macko, S.A., Engel, M.E., and Parker, P.L., 1993. Early diagenesis of organic matter in sediments: assessment of mechanisms and preservation by the use of isotopic molecular approaches. *In* Engel, M.A., and Macko, S.A. (Eds.), *Organic Geochemistry Principals and Applications.* New York (Plenum), 211–224.

Macko, S.A., and Estep, M.L.F., 1984. Microbial alteration of stable nitrogen and carbon isotopic compositions of organic matter. *Org. Geochem.,* 6:787–790. **doi:10.1016/0146-6380(84)90100-1**

Macko, S.A., Estep, M.L.F., Hare, P.E., and Hoering, T.C., 1983. Stable nitrogen and carbon isotopic composition of individual amino acids isolated from cultured microorganisms. *Year Book, Carnegie Institution of Washington,* 82:404–410.

Macko, S.A., Estep, M.L.F., Engel, M.H., and Hare, P.E., 1986. Kinetic fractionation of stable nitrogen isotopes during amino acid transamination. *Geochim. Cosmochim. Ac*ta, 50(10):2143–2146. **doi:10.1016/0016-7037(86)90068-2**

Pontoizeau, P., Castanier, S., and Perthuisot, J.P., 1996. Bacterial production of struvite ($MgNH_4PO_4{\cdot}6H_2O$) during experiments aiming to produce high-Mg carbonates. *Comptes Rendus Academie Sciences Serie Fascicule a-Sciences Terre Des Planetes,* 323(2):121–28.

Pride, C., Thunell, R., Sigman, D., Keigwin, L., Altabet, M., and Tappa, E., 1999. Nitrogen isotopic variations in the Gulf of California since the last deglaciation: response to global climate change. *Paleoceanography,* 14(3):397–409. **doi:10.1029/1999PA900004**

Prokopenko, M.G., Hammond, D.E. Berelson, W.M., Bernhard, J.M., Stott, L., and Douglas, R., 2006. Nitrogen cycling in the sediments of Santa Barbara Basin and eastern subtropical North Pacific: nitrogen isotopes, diagenesis and possible chemosymbiosis between two lithotrophs (Thioploca and Anammox)—"riding on a glider." *Earth Planet. Sci. Lett.,* 242(1–2):186–204. **doi:10.1016/j.epsl.2005.11.044**

Prokopenko, M.G., 2004. Fractionation of nitrogen isotopes during early diagenesis [Ph.D. thesis]. Univ. Southern California, Los Angeles.

Prokopenko, M.G., Hammond, D.E. and Stott, L., in press. Lack of isotopic fractionation of ^{15}N of organic matter during long-term diagenesis in marine sediments; ODP Leg 202–Sites 1234 and 1235. *In* Tiedemann, R., Mix, A.C., Richter, C., and Ruddiman, W.F. (Eds.), *Proc. ODP, Sci. Results*, 202. College Station TX (Ocean Drilling Program).

Redfield, A.C., Ketchum, B.H., and Richards, F.A., 1963. The influence of organisms on the composition of seawater. *In* Hill, M.N. (Ed.), *The Sea* (Vol. 2): New York (Wiley), 26–77.

Rivadeneyra, M.A., Martin-Algarra, A., Sanchez-Navas, A., and Martin-Ramos, D., 2006. Carbonate and phosphate precipitation by *Chromohalobacter marismortui. Geomicrobiol. J.,* 23(2):89–101. **doi:10.1080/01490450500533882**

Sachs, J.P., and Repeta, D.J., 1999. Oligotrophy and nitrogen fixation during eastern Mediterranean sapropel events. *Science,* 286(5449):2485–2488. **doi:10.1126/science.286.5449.2485**

Sigman, D.M., 1997. The role of biological production in Pleistocene atmospheric carbon dioxide variations and the nitrogen isotope dynamic of the Southern Ocean, Ph.D. Thesis., MIT/WHOI, 97–28.

Sigman, D.M., Altabet, M.A., Francois, R., McCorkle, D.C., and Gaillard, J.-F., 1999. The isotopic composition of diatom-bound nitrogen in the Southern Ocean sediments. *Paleoceanography,* 14(2):118–134. **doi:10.1029/1998PA900018**

Sigman, D.M., Altabet, M.A., Michener, R., McCorkle, D.C., Fry, B., and Holmes, R.M., 1997. Natural abundance-level measurement of the nitrogen isotopic composition of oceanic nitrate: an adaptation of the ammonia diffusion method. *Mar. Chem.,* 57(3-4):227–242. **doi:10.1016/S0304-4203(97)00009-1**

Sigman, D.M., and Boyle, E.A., 2000. Glacial/interglacial variations in atmospheric carbon dioxide. *Nature (London, U. K.),* 407(6806):859–869. **doi:10.1038/35038000**

Silfer, J.A., Engel, M.H., and Macko, S.A., 1992. Kinetic fractionation of stable carbon and nitrogen isotopes during peptide bond hydrolysis: experimental evidence and geochemical implications. *Chem. Geol.*, 101:211–221.

Sorensen, P., and Jensen, E.S., 1991. Sequential diffusion of ammonium and nitrate from soil extracts to a polytetrafluoroethylene trap for N-15 determination. *Anal. Chim. Acta,* 252(1–2):201–203. **doi:10.1016/0003-2670(91)87215-S**

Suess, E., von Huene, R., et al., 1988. *Proc. ODP, Init. Repts.,* 112: College Station, TX (Ocean Drilling Program).

Sweeney, R.E., and Kaplan, I.R., 1980. Natural abundances of ^{15}N as a source indicator for near-shore marine sedimentary and dissolved nitrogen. *Mar. Chem.,* 9(2):81–94. **doi:10.1016/0304-4203(80)90062-6**

Tyrell, T., 1999. The relative importance influences of nitrogen and phosphorus on oceanic primary production. *Nature (London, U. K.),* 400(6744):525–531. **doi:10.1038/22941**

Figure F1. Map of locations for Leg 201, Sites 1227 and 1230.

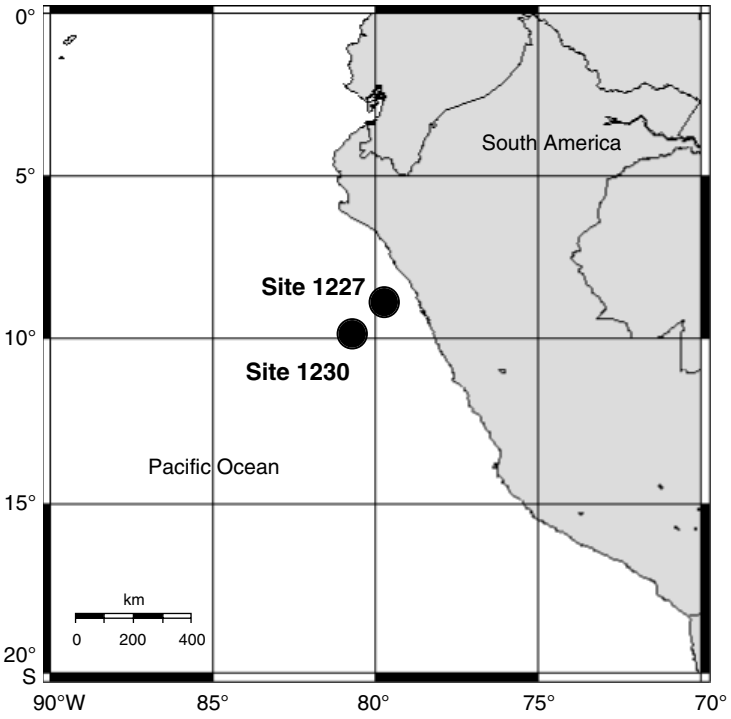

Figure F2. Site 1230 total organic carbon (TOC) and total nitrogen (TN) concentrations in the sediments (dashed line represents boundary between different lithologic units).

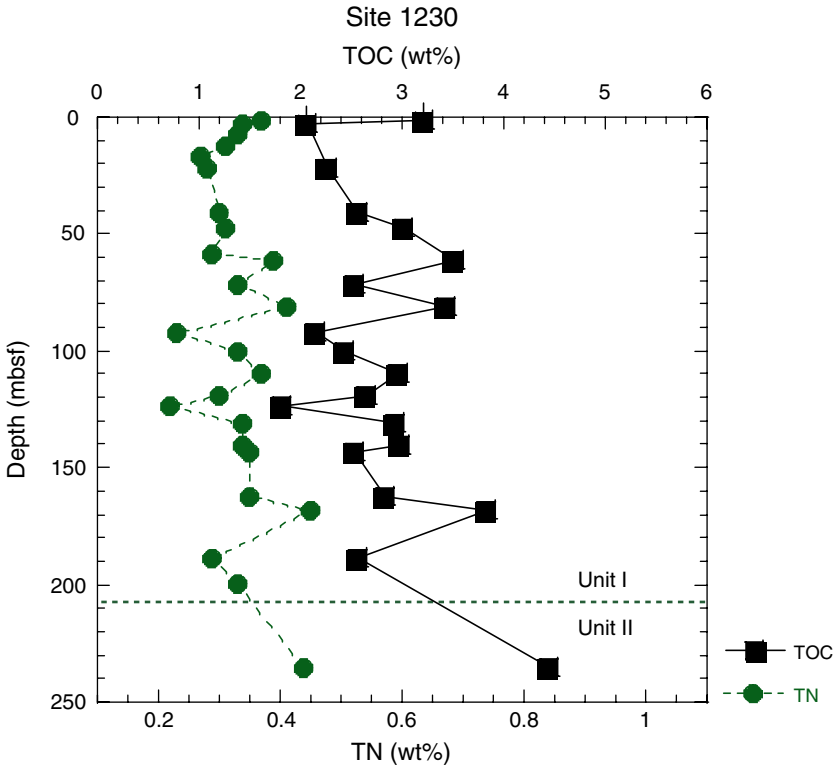

Figure F3. Site 1230 ammonium profile, $\delta^{15}N$ of ammonium and bulk sediments (dashed line represents boundary between different lithologic units' error bar = 0.7‰).

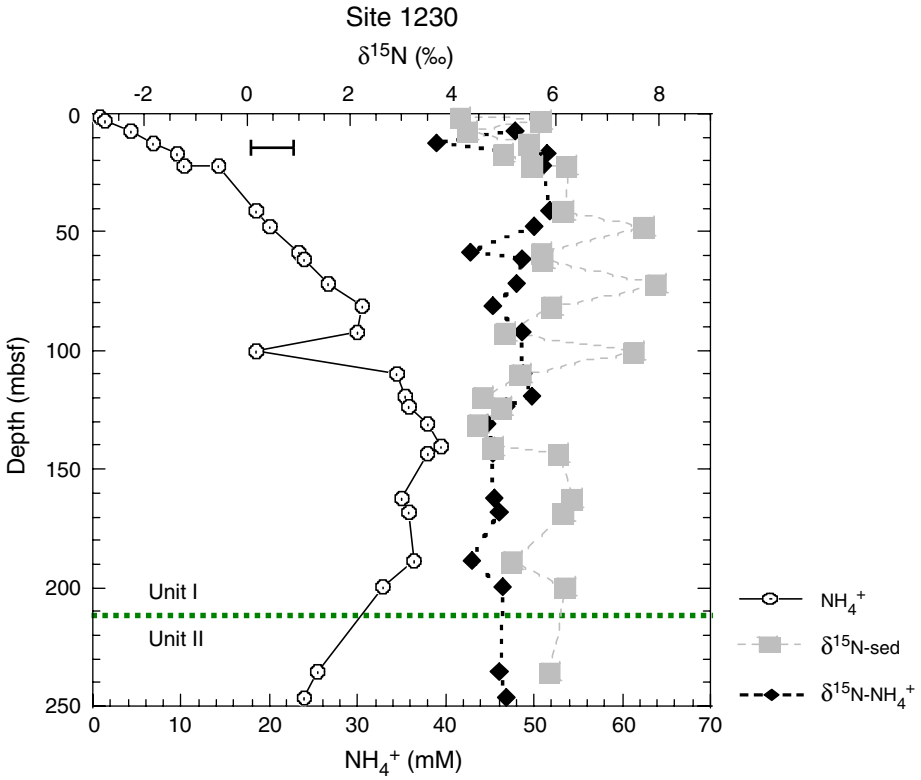

Figure F4. Pore water sulfate profile at Site 1227 (D'Hondt, Jorgensen, Miller, et al., 2003).

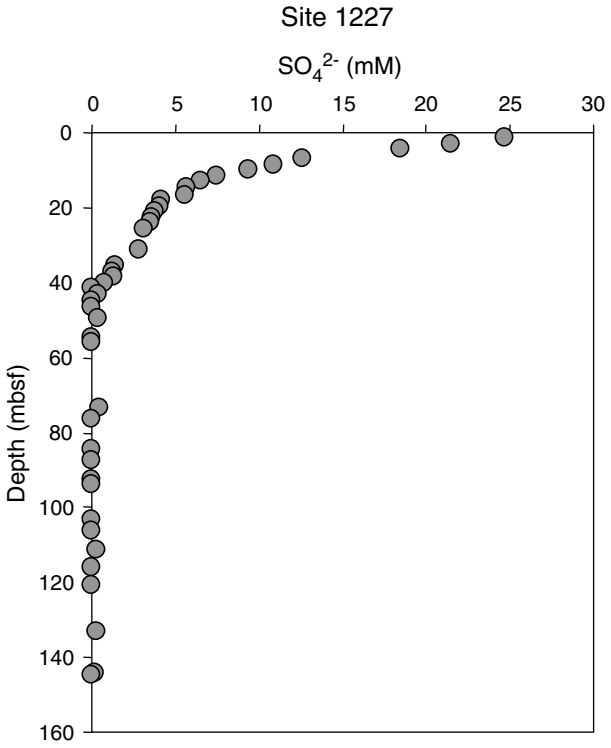

Figure F5. Isotopic composition of pore water ammonium bulk sediments and ammonium concentrations, Site 1227 (dashed lines represent boundaries between lithologic units).

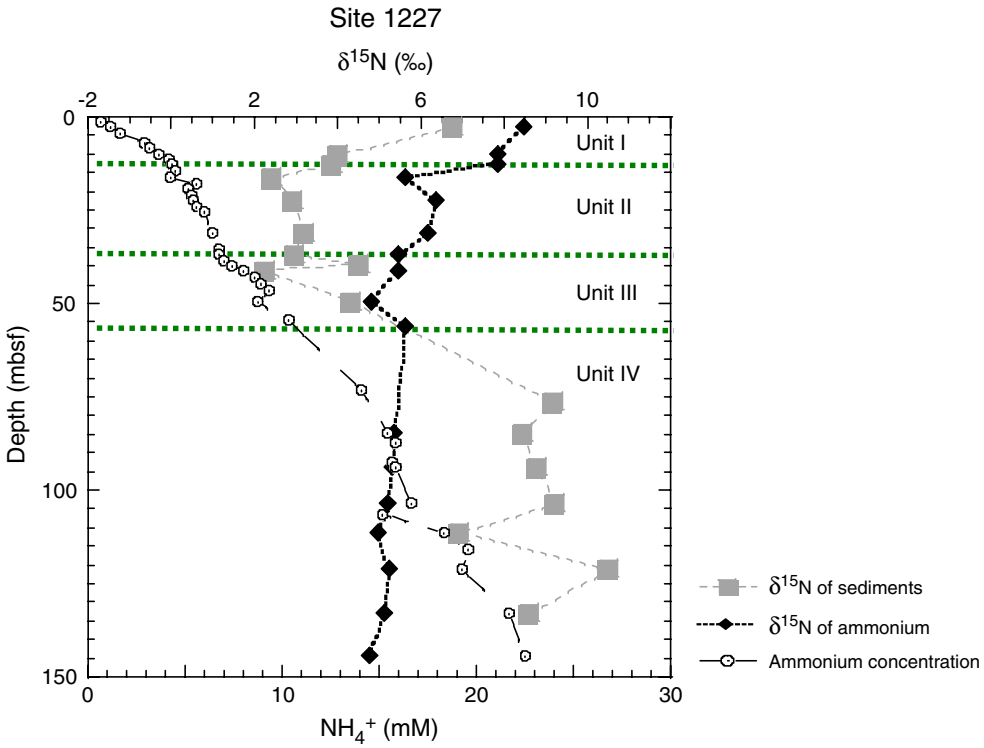

Figure F6. Concentrations of pore water chloride and ammonium, Site 1227 (D'Hondt, Jorgensen, Miller et al., 2003).

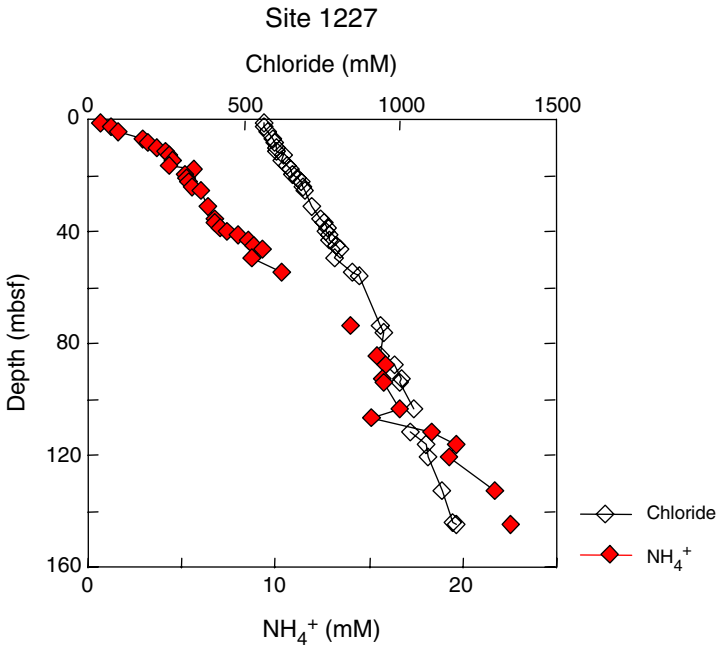

Figure F7. Site 1227 total organic carbon (TOC) and total nitrogen (TN) concentrations of the sediments (dotted lines represent boundaries of lithologic units).

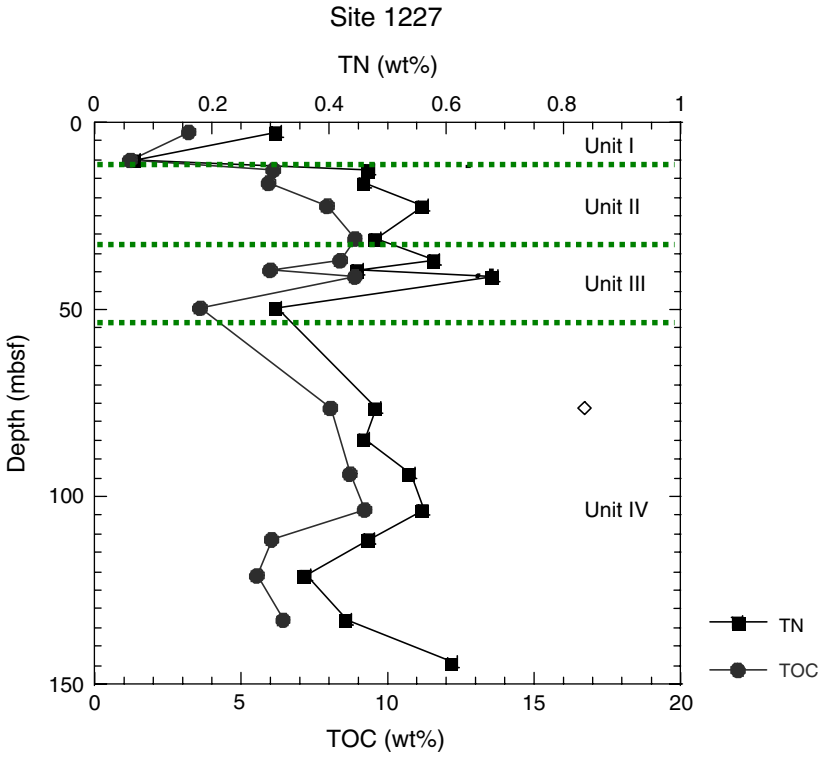

Figure F8. Ammonium vs. chloride concentrations in the pore water of Site 1227; note the "kink" at 36–38 mbsf. Line A represents simple mixing between the brine and seawater; Line B represents the effect of N_{org} decomposition on the mixing pattern between seawater and the brine.

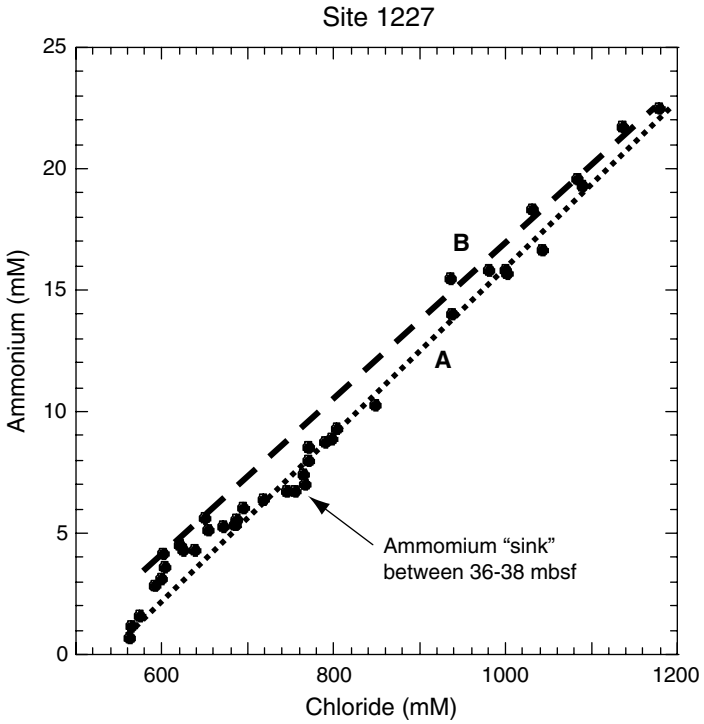

Figure F9. Site 1227 mixing diagram (the parenthesis around one data point indicate that the measured value may be questionable). Shaded circle designates the interval associated with the apparent sink.

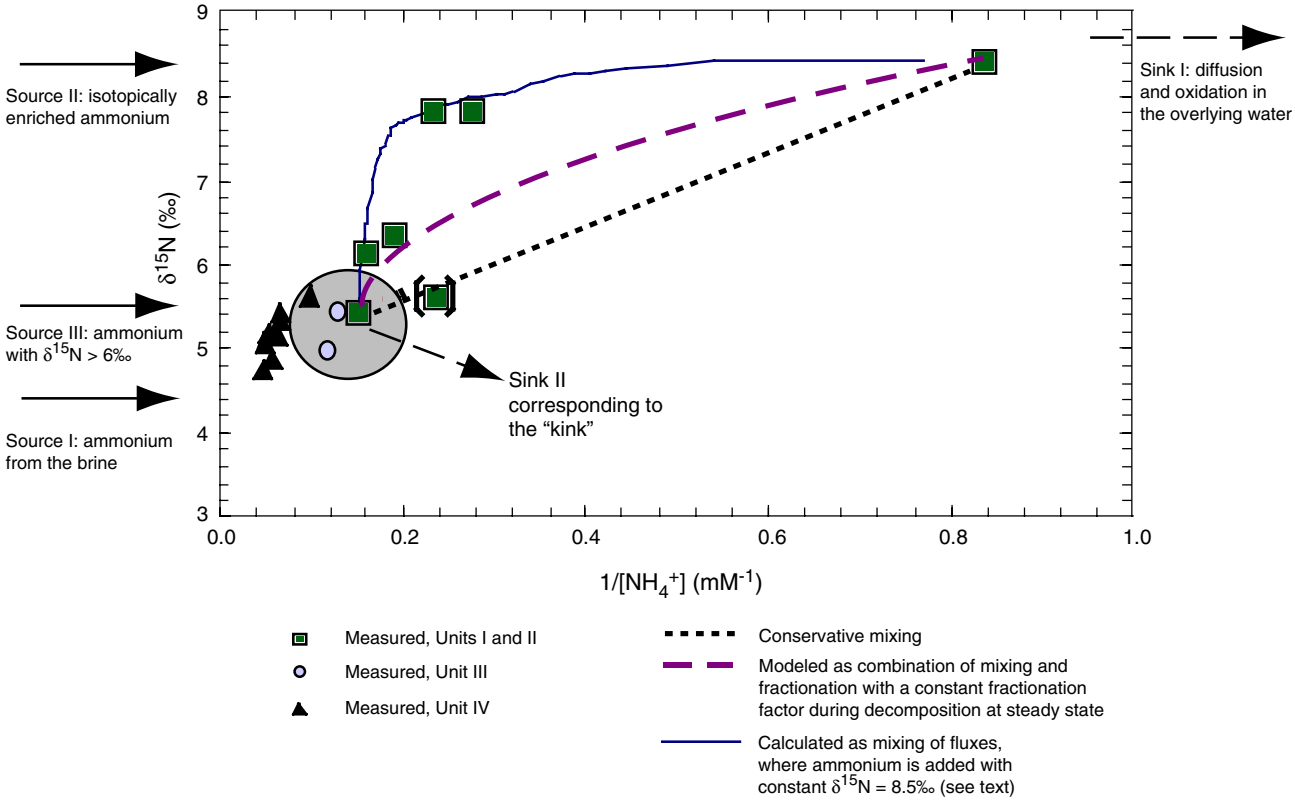

Figure F10. Site 1227 schematic representation of ammonium fluxes and $\delta^{15}N$ of the fluxes calculated with the assumption that ammonium profile is in a steady state (fluxes are in mol/cm^{2}yr).

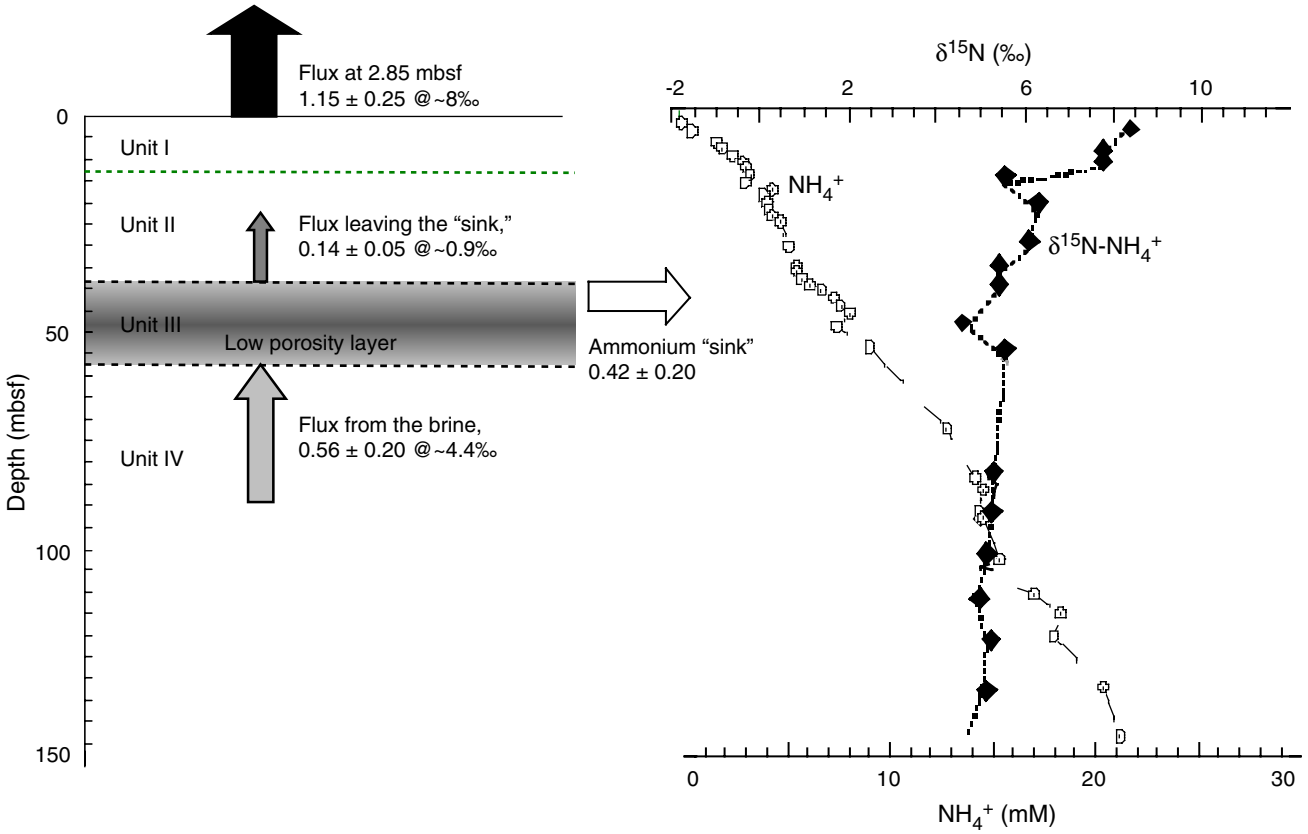

Table T1. Sediment elemental composition, ammonium concentration, and $\delta^{15}N$ of sediments and pore water ammonium, Hole 1230A.

Core, section, interval (cm)	Depth (mbsf)	TOC (wt%)	TN (wt%)	C/N ratio atomic	$[NH_4^+]$* (mM)	$\delta^{15}N$ (‰) Pore water	$\delta^{15}N$ (‰) Sediment
201-1230A-							
1H-1, 135–150	1.35	3.22	0.37	10.1	0.78	NA	4.17
1H-2, 135–150	2.85	2.07	0.34	7.1	1.34	NA	5.72
2H-2, 135–150	7.65	NA	0.33	NA	4.32	5.19	4.31
2H-5, 135–150	12.15	NA	0.31	NA	6.85	3.67	5.49
3H-2, 135–150	17.15	NA	0.27	NA	9.57	5.84	5
3H-5, 135–150	21.65	2.26	0.26	10.2	10.25	5.72	6.24
5H-5, 135–150	40.65	2.56	0.3	10	18.47	5.88	6.18
6H-3, 143–158	47.23	3.01	0.31	11.3	19.95	5.57	7.73
8H-3, 135–150	58.65	NA	0.29	NA	23.31	4.32	5.73
8H-5, 135–150	61.65	3.51	0.39	10.5	23.99	5.33	5.78
10H-1, 135–150	71.65	2.53	0.33	9	26.65	5.22	7.96
11H-1, 135–150	81.15	3.44	0.41	9.8	30.5	4.78	5.93
12H-2, 135–150	92.15	2.15	0.23	10.9	29.98	5.33	5.05
13H-1, 135–150	100.15	2.44	0.33	8.6	18.42	NA	7.53
14H-1, 135–150	109.65	2.96	0.37	9.3	34.35	5.37	5.33
15H-2, 135–150	119.47	2.65	0.3	10.3	35.43	5.52	4.61
15H-5, 85–98	123.47	1.81	0.22	9.6	35.87	5.03	4.98
17H-1, 135–150	130.65	2.93	0.34	10.1	37.84	4.67	4.5
18H-2, 0–20	141.65	2.98	0.34	10.2	39.41	4.79	4.81
18H-4, 0–20	143.3	2.54	0.35	8.5	37.88	4.78	6.07
21H-4, 69–84	162.47	2.83	0.35	9.4	34.99	4.8	6.33
22H-1, 75–90	169.05	3.83	0.45	9.9	35.79	4.91	6.17
24H-2, 0–98	188.8	2.56	0.29	10.3	36.43	4.38	5.18
26H-1, 82–97	199.6	NA	0.33	NA	32.96	4.98	6.2
33X-1, 130–150	235.7	4.45	0.44	11.8	25.41	4.9	5.89
35X-1, 136–156	246.4	NA	NA	NA	23.87	5.03	NA

Notes: * = measured at USC. NA = not available.

Table T2. Parameters for modeling ammonium profiles and modeling results, Sites 1230 and 1227.

	Site 1230	Site 1227
Specified parameters:		
ϕ: average porosity	0.75	0.6–0.8
D_s: diffusivity (cm^2/s)*	7.5×10^{-6}	5.35×10^{-6} to 8.12×10^{-6}
w: accumulation rate (cm/s)	3.17×10^{-10}	6.34×10^{-11}
K: ammonium adsorption coefficient†	1.3	1.3
Peclet number	3	54
ρ: density of solid phase (g/cm^3)	2.4	2.4
Fitted parameters:		
β: inverse of scale distance (m^{-1})	0.0268 ± 0.0015	0.0667 ± 0.0046
A1: integration constant ($\mu mol/cm^3$)	19.2	6.7
Calculated parameters:		
N_{org} lost via decomposition (wt%)	0.98 ± 0.10	1.10 ± 0.15

Notes: * = corrected for tortuosity: $D_m/\{1 - [\ln(por2)]\}$, where D_m = molecular diffusion at 5°C, 11.75 cm^2/s (Boudreau, 1997; Li and Gregory, 1974). † = adsorption coefficient typical for coastal sediments (Berner, 1980). Peclet number = $D_s \times \beta/[(1 + K) \times w]$.

Table T3. Sediments elemental composition and $\delta^{15}N$ for sediments and pore water ammonium, Hole 1227A.

Core, section, interval (cm)	Depth (mbsf)	TOC (wt%)	TN (wt%)	C/N atomic	$[NH_4^+]$* (mM)	$\delta^{15}N$ (‰)	
						Pore water	Sediment
201-1227A-							
1H-2, 135–150	2.85	3.21	0.31	12.3	1.25	8.45	7.42
2H-3, 135–150	9.95	1.25	0.07	20.7	3.54	7.84	3.84
2H-5, 135–150	12.95	6.11	0.47	15.2	5.12	7.84	3.83
3H-1, 135–150	16.45	5.93	0.46	15.1	4.45	5.63	2.57
3H-5, 135–150	22.45	7.97	0.56	16.5	5.81	6.38	2.6
4H-5, 95–110	31.21	8.89	0.48	21.5	5.96	6.17	2.25
5H-2, 135–150	36.95	8.38	0.58	17	6.38	5.46	2.12
5H-4, 135–150	39.35	6.02	0.45	15.7		NA	4.46
5H-5, 135–150	41.45	8.87	0.68	15.2	7.65	5.48	2.43
6H-4, 135–150	49.95	3.6	0.31	13.7	8.61	5.01	3.93
7H-2, 135–150	55.95	NA	NA	NA	9.14	5.66	NA
9H-3, 135–150	76.45	8.05	0.48	19.5	NA	NA	9.36
10H-2, 135–150	84.45	NA	0.46	NA	15.51	5.35	8.46
11H-2, 135–150	93.95	8.75	0.54	18.9	15.77	5.45	9.42
12H-2, 135–150	103.45	9.25	0.56	19.1	16.65	5.18	9.55
13H-1, 135–150	111.45	6.05	0.47	15	18.03	4.9	7.18
14H-1, 135–150	120.95	5.57	0.36	17.9	19.21	5.23	10.44
17H-1, 85–90	132.95	6.42	0.43	17.2	20.91	5.09	9.33
18H-2, 135–150	144.3	NA	0.61	NA	22.49	4.77	8.35

Notes: * = measured at USC. NA = not available.